

# Spatially Resolved IR Microspectroscopy of Single Cells

PETER LASCH,\* ANTHONY PACIFICO, MAX DIEM

Departments of Chemistry and Biochemistry, Hunter College and Graduate Center of the City University of New York, 695 Park Avenue, New York, New York 10021

Received 8 September 2001; revised 6 November 2001; accepted 19 November 2001

Published online 26 April 2002 in Wiley InterScience (www.interscience.wiley.com). DOI: 10.1002/bip.10095

**ABSTRACT:** Fourier transform IR (FTIR) microspectroscopy at a spatial resolution of 18  $\mu\text{m}$  was used to study skin fibroblasts and giant sarcoma cells. Both cell lines were derived from the same patient; they were metabolically active and in the exponentially growing phase. The IR spectra were acquired for the nuclei and cytosol of untreated cells, cells washed with ethanol, and cells treated with RNase or DNase. A comparison of the spectra of the two cell lines yielded only insignificant spectral differences, indicating that IR spectroscopy monitors the overall cell activity rather than specific signs of cancer. © 2002 Wiley Periodicals, Inc. *Biopolymers (Biospectroscopy)* 67: 335–338, 2002

**Keywords:** biomedical spectroscopy; Fourier transform IR microspectroscopy; single cell spectroscopy

## INTRODUCTION

Fourier transform IR (FTIR) microspectroscopy uses IR radiation to detect the molecular chemistry of microscopic samples. In the last years this technique has become a useful nondestructive and reagent-free tool in analytical chemistry, material science, biology, and medicine. For instance, many research groups have been involved in applying microspectroscopy to a number of problems in tissue research with particular emphasis on detecting spectral differences between normal and malignant tissue structures.<sup>1–5</sup> These groups documented for a number of distinct organs that IR spectroscopy can be used to detect tissue malignancies. Many of the authors ob-

served subtle spectral changes between normal and malignant tissue samples, particularly for the symmetric and antisymmetric  $\text{—PO}_2$  bands (1088 and 1234  $\text{cm}^{-1}$ ), which typically appear in the IR spectra of nucleic acids, phospholipids, and phosphorylated proteins. In order to systematically investigate the spectral alterations associated with carcinogenesis and tumor progression we initiated a research program on well-characterized cell lines. To this end, we developed a method for growing cells directly on IR transparent materials and collecting separate IR spectra from the nucleus and the cytoplasm. The IR measurements were carried out on cells that were consecutively treated by ethanol, RNase and DNase to remove cellular phospholipids, RNA, or DNA, respectively.

Correspondence to: P. Lasch (laschp@rki.de).

\*Present address: Robert Koch-Institut, P34 Biophysical Structure Analysis, Nordufer 20, 13353 Berlin, Germany.

Contract grant sponsor: American Cancer Society; contract grant number: ROG 99-119-01.

Contract grant sponsor: NIH (to M.D.); contract grant numbers: CA 81675; GM 60654.

Contract grant sponsor: National Center for Research Resources of the NIH; contract grant number: RR-03037.

*Biopolymers (Biospectroscopy)*, Vol. 67, 335–338 (2002)  
© 2002 Wiley Periodicals, Inc.

## MATERIALS AND METHODS

Cell cultures of human skin fibroblasts (CRL-7553) and giant sarcoma cells (CRL-7554) were purchased from the American Type Culture Collection (ATCC, Manassas, VA) and were cultured

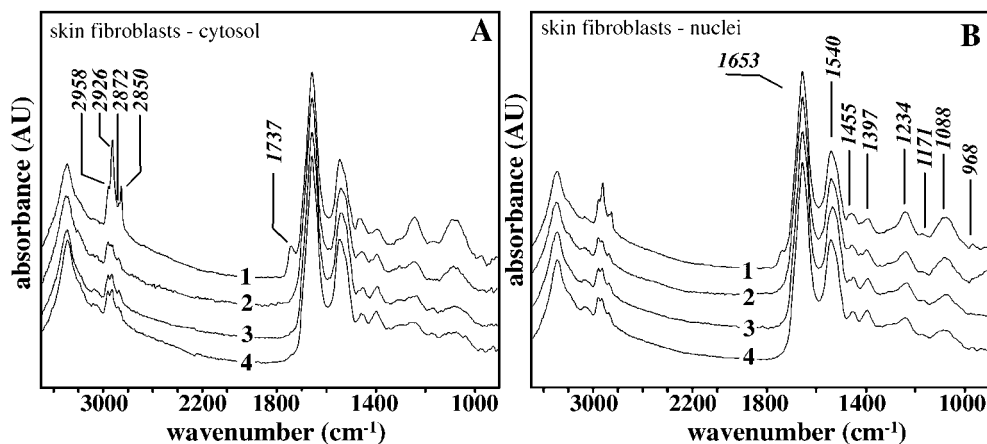


**Figure 1.** IR microspectra of (A) cytoplasm and (B) nuclei of human skin fibroblasts. Traces 1 are the untreated cells; traces 2 are after ethanol treatment for removal of lipids; traces 3 are after ethanol treatment and RNase digestion; and traces 4 are after ethanol treatment and RNase and DNase digestion. The aperture size is  $18 \times 18 \mu\text{m}^2$ . The spectra are averaged (about 20 individual cells) and normalized in the amide I band ( $1620\text{--}1690 \text{ cm}^{-1}$ ).

according to standard procedures. The cells were grown directly on 1-mm thick  $\text{CaF}_2$  windows to which they attach strongly. Subsequently, the windows were washed with distilled water to remove growth medium and air dried.

#### Ethanol, RNase, and DNase Treatment

Cells on the  $\text{CaF}_2$  substrates were exposed for 5 min to 96% ethanol (Fisher Scientific). Some of the alcohol treated specimens were subsequently incubated twice with RNase A solutions (1 mg/mL, Sigma) for 15 min at  $37^\circ\text{C}$ . Finally, some specimens were digested with DNase (1 mg/mL, Sigma) for 15 min at  $37^\circ\text{C}$ .

#### IR Measurements

The measurements were carried out using an IR-Scope II IR microscope coupled to a Vector22 FTIR spectrometer (Bruker Optics, Billerica, MA). The IR microscope is equipped with a single HgCdTe (MCT) detector and a computer controlled microscope stage. The experimental setup permitted spectral data to be collected using an optical aperture of  $18 \times 18 \mu\text{m}^2$ . Spectra were collected at  $8 \text{ cm}^{-1}$  resolution. Mapping data were analyzed using software developed in house. This software will be described in more detail at a later date and is available for distribution.<sup>6</sup>

## RESULTS

#### IR Spectra of Skin Fibroblasts

Figure 1(A,B) shows the IR spectra of the cytosol and the nuclei, respectively, of human skin fibroblasts. Each spectrum of Figure 1 is an average spectrum obtained from about 20 individual cells. The most striking differences between the spectra from nuclei and cytosol of untreated skin fibroblasts (trace 1) can be found in the C—H stretching region ( $2800\text{--}3050 \text{ cm}^{-1}$ ) and at  $1737 \text{ cm}^{-1}$  ( $\text{C}=\text{O}_{\text{ester}}$ ), indicating considerably higher phospholipid concentrations for the cytosol. This is consistent with earlier observations in which we analyzed IR spectra from defined cell fractions produced by differential centrifugation.<sup>7</sup> We believe that the observed phospholipid features are due to intracellular organelles such as the endoplasmic reticulum, mitochondria, or the Golgi apparatus, rather than from the cellular membrane.

The ethanol treated cells (Fig. 1, trace 2) exhibit spectra devoid of the  $\text{C}=\text{O}_{\text{ester}}$  peak at  $1737 \text{ cm}^{-1}$ , indicating virtually complete removal of phospholipids. This statement is backed by the observation of diminished band intensities in the C—H stretching region ( $2800\text{--}3050 \text{ cm}^{-1}$ ). Additional spectral alterations can be observed in the low frequency region ( $1000\text{--}1500 \text{ cm}^{-1}$ ), particularly for the symmetric and antisymmetric  $\text{—PO}_2^-$  bands at 1088 and  $1234 \text{ cm}^{-1}$ . In the spectra of

ethanol treated cells these bands are more pronounced for the nuclei, demonstrating higher concentrations of  $\text{—PO}_2^-$  groups (contained, e.g., in DNA, RNA, and phosphorylated proteins) in the nuclei.

Treating the ethanol-washed samples with RNase further enhances the spectral differences between the nuclei and cytoplasm (Fig. 1, trace 3). This step removes most of the RNA in the cytoplasm and most of the nuclear RNA. The remaining bands at 1088 and 1234  $\text{cm}^{-1}$  in the spectra of the nuclei [Fig. 1(B), trace 3] are thus due to nuclear DNA. Final digestion of the skin fibroblast cells with DNase did not reveal a further decrease of the  $\text{—PO}_2^-$  bands (Fig. 1, cf. traces 3 and 4). This may indicate that the nuclear DNA was inaccessible to DNase.

### Spectral Comparison of Skin Fibroblasts and Giant Sarcoma Cells

The cells whose spectra are compared in Figure 2 (benign skin fibroblasts and malignant giant sarcoma cells) were derived from the same patient. In the low frequency region (1000–1500  $\text{cm}^{-1}$ , see Fig. 2) these spectra display subtle differences between the cell lines and between the nuclei and the cytosol. These differences can be mainly attributed to variations of the phospholipid content (cf. the C—H stretching region 2800–3050  $\text{cm}^{-1}$  and the  $\text{C=O}_{\text{Ester}}$  band at 1737  $\text{cm}^{-1}$ ). Interestingly, the phospholipid content of skin fibroblasts is generally higher than giant sarcoma cells (see

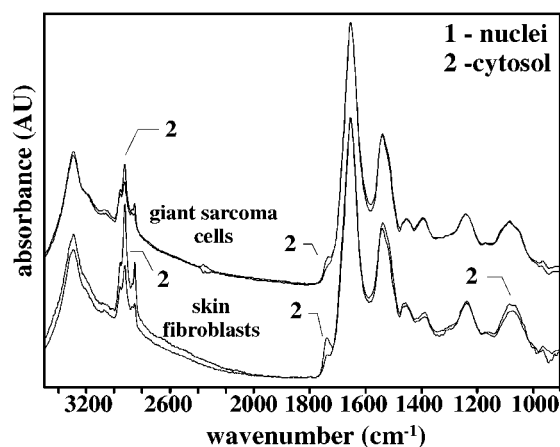


**Figure 2.** IR microspectra of giant sarcoma cells (top traces) and skin fibroblasts (bottom traces) for nuclei (traces 1) and cytosol (traces 2). All spectra are normalized average spectra. The aperture size is  $18 \times 18 \mu\text{m}^2$ .

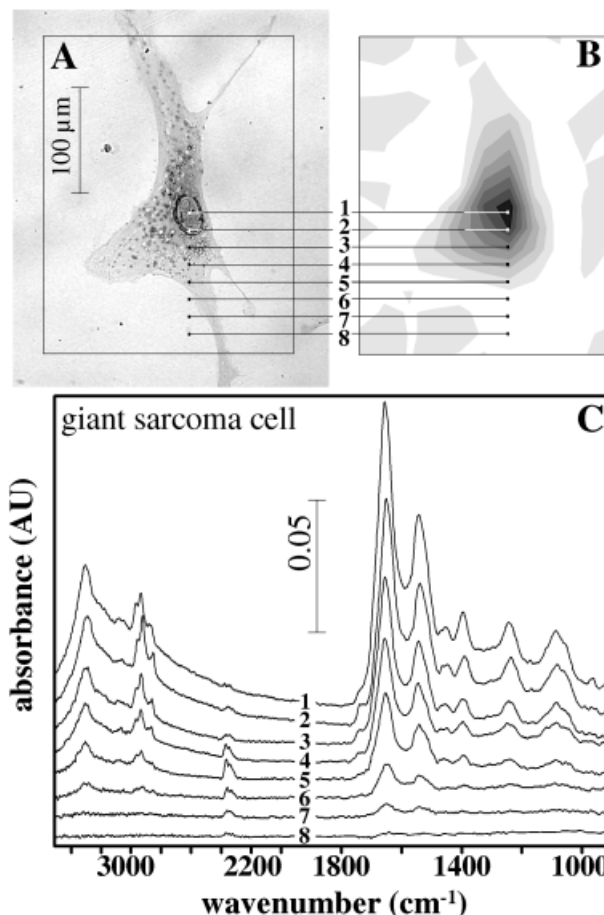


**Figure 3.** A photomicrograph of an unstained dry giant sarcoma cell. The nucleus appears as a large dark spot in the center of the cell. (A) An IR map of the cell shown, constructed from gray scale values corresponding to the integrated absorbance of the amide I band (1620–1680  $\text{cm}^{-1}$ ). The sample area is  $200 \times 300 \mu\text{m}$ , the step size is  $20 \mu\text{m}$ , the aperture size is  $25 \times 25 \mu\text{m}^2$ , and there are 176 pixels. (A,B) The IR spectra from positions 1–8 are indicated.

$\text{C=O}_{\text{Ester}}$  band at 1737  $\text{cm}^{-1}$ ). These results are important for the interpretation of the phosphate-stretching bands, which are superpositions of various  $\text{—PO}_2^-$  subbands arising from phosphodiester groups of species such as DNA, RNA, phospholipids, phosphorylated proteins, and inorganic phosphate.

### Spectral Map of Giant Sarcoma Cell

We now turn to the discussion of an IR spectral map of a giant sarcoma cell. Figure 3(A) displays a microphotograph of an unstained sarcoma cell measuring over  $200 \mu\text{m}$  along its largest dimen-

sion. The cell exhibits a large nucleus and a typical fibroblast-like shape of the cell body. Spatially resolved IR spectra were acquired from the untreated cell using the parameters listed in the caption to Figure 3. The image shown in Figure 3(B) was assembled using the integrated absorbance of the amide I band between 1620 and 1680  $\text{cm}^{-1}$ ; thus, this map shows the protein distribution in the cell. The dark spot in the center of Figure 3(B) indicates high absorbances whereas regions with low readings of absorbance for the amide I band are white. The nucleus exhibits the largest protein signals, which are due to either the largest protein concentration or the longer pathlength the IR beam travels through the sample or both. Figure 3(A,B) also depicts the positions at which the spectra displayed in Figure 3(C) were acquired. These spectra were extracted from the mapping data along a trace starting near the center of the nucleus [Fig. 3(C), spectrum 1] and ending outside the cell (spectrum 8). According to Figure 3(C), the concentration of phospholipids is highest in the region immediately surrounding the nucleus, in agreement with the data shown in Figures 1 and 2.

## DISCUSSION

In earlier studies we presented IR spectra that exhibit relatively high IR absorptions in the phosphate-stretching region for cells in the S phase (where DNA is replicated), whereas cells in other phases show very low phosphate signals. The inability to detect the nuclear DNA in the G1/G2 phases was attributed to the enormously dense packing of DNA in condensed chromatin, which can produce such a large local absorbance for nucleosomes that they are unobservable.<sup>8</sup> It was also concluded that in these phases most of the IR nucleic acid signals are due to RNA.

This conclusion was corroborated by spatially resolved IR microspectroscopy of oral mucosa cells, where we found very low and nearly identical phosphate absorptions in the spectra of nuclei and the cytosol.<sup>7</sup> Because oral mucosa cells are fully differentiated and metabolically inactive, these findings supported the aforementioned hypothesis of the "invisibility" of densely packed nuclear DNA.

In this article we extend the spatially resolved IR studies for single cells. We present data obtained at high spatial resolution of skin fibro-

blasts and giant sarcoma cells, which both exhibit high levels of metabolic and divisional activity. It was expected that DNA is partly uncoiled during replication and is hence detectable. In order to be able to differentiate between the phosphate signals from lipids (phospholipids), RNA, and DNA, all experiments were carried out on cell samples treated with alcohol, RNase, and DNase. Indeed, we find that small DNA signals are detected in the nuclei after removal of other sources of phosphate groups.

Furthermore, we report for the first time large signals of phospholipid in the cytoplasm and large cytoplasmic RNA signals. Both these components appear to be observed only in physiologically active cells.

The data of this study support the hypothesis that IR microspectroscopy of tissues monitors the level of cell activity rather than signatures specific to cancer. Furthermore, it appears that the higher the cell's divisional and metabolic activity, the more pronounced the  $-\text{PO}_2^-$  bands of DNA, RNA, and phospholipids will be. The experimental data of the present study also support the hypothesis that condensed DNA of inactive (pyknotic) nuclei is invisible to IR transmission spectroscopy.

Support of this research through grants from the American Cancer Society, the NIH, and from a Research Centers in Minority Institutions (National Center for Research Resources of the NIH) are gratefully acknowledged.

## REFERENCES

1. McIntosh, L. M.; Jackson, M.; Mantsch, H. H.; Stranc, M. F.; Pilavdzic, D.; Crowson, A. N. *J Invest Dermatol* 1999, 112, 951.
2. Fabian, H.; Jackson, M.; Murphy, L.; Watson, P. H.; Fichtner, I.; Mantsch, H. H. *Biospectroscopy* 1995, 1, 37–45.
3. Lasch, P.; Naumann, D. *Cell Mol Biol* 1998, 44, 189–202.
4. Andrus, P. G. L.; Strickland, R. D. *Biospectroscopy* 1998, 4, 37–46.
5. Diem, M.; Boydston-White, S.; Chiriboga, L. *Appl Spectrosc* 1999, 53, 148A–161A.
6. Available from <http://www.cytospec.com>.
7. Lasch, P.; Boese, M.; Pacifico, A.; Diem, M. *Vibrat Spectrosc*, to appear.
8. Chiriboga, L.; Xie, P.; Yee, H.; Zarou, D.; Zakim, W.; Diem, M. *Cell Mol Biol* 1999, 44, 219–229.